

Performance of Highly Mobile Cognitive Radio Networks with Directional Antennas

Robert Murawski and Eylem Ekici
 Department of Electrical and Computer Engineering
 The Ohio State University
 Columbus, Ohio 43210
 Email: {murawskr,ekici}@ece.osu.edu

Vasu Chakravarthy and William K. McQuay
 Air Force Research Laboratory
 2241 Avionics Cir.
 Wright-Patterson AFB OH 45433
 Email: {Vasu.Chakravarthy,william.mcquay}@wpafb.af.mil

Abstract—Cognitive radio systems allow secondary users to operate on underutilized licensed spectrum. When considering highly congested communication channels, however, opportunities for channel access based on time or frequency division can be limited for secondary user networks. In this research, we consider leveraging enhanced spatial diversity through directional steerable antennas to allow secondary user channel access in parallel with licensed spectrum users. Furthermore, we consider effects of mobility on directional secondary user networks and introduce a mechanism for maintaining point-to-point directional communication links in the presence of mobility. We study the trade-offs between spatial diversity and coordination overhead to motivate the use of directional antennas, even in highly mobile cognitive radio networks.

Index Terms—Cognitive Radio, Dynamic Spectrum Access, Directional Antenna

I. INTRODUCTION

It is well-known that the unlicensed portions of the spectrum are subject to much congestion in highly populated areas. At the same time, studies by the Federal Communications Commission (FCC) [1] have shown that the licensed portions of the spectrum, while generally reserved, are used sparsely with respect to both time and location. Cognitive radio systems [2], [3] can increase the utilization of the wireless spectrum by allowing unlicensed users to non-intrusively utilize the licensed portion of the spectrum. A survey of cognitive radio networks (CRNs) can be found in [4].

While utilizing licensed spectrum can potentially alleviate congestion, it must be done while maintaining the integrity of the local licensed users. This is typically accomplished through traditional medium access control (MAC) technologies such as: FDMA [5], TDMA [6], CDMA [7], or some other variant. The authors in [8] showed when the traditional resources are not readily available, by working cooperatively with primary users (PUs), secondary users (SUs) can still utilize licensed channels. However, when utilizing highly congested channels with uncooperative PUs, other means of isolation from PUs must be explored.

Advanced antenna designs have been widely studied in the context of wireless sensor networks [9], [10], ad-hoc networks [11], [12], and the like. Directional steerable antennas can be utilized to focus the main energy of a transmission in a desired direction, while significantly limiting the interference gener-

ated in all other directions. In the context of cognitive radio networks, we can utilize these antennas to limit interference in the direction of primary licensed spectrum users. Thus, for a network of directional secondary users, more communication paths can be available as the interference in the direction of primary users is reduced.

The benefits of utilizing directional antennas for static networks of secondary users has been shown in [13]. For mobile networks, additional overhead is required for coordination among SUs to maintain accurate directional information. As users move in the network, this information must be refreshed to maintain communications. We build on our previous research in the area of neighborhood discovery [14] to introduce a means of refreshing neighborhood information. As the beamwidth of the antennas is decreased, we will show that the coordination overhead for maintaining neighbor information increases. However, due to increased spatial diversity of the narrower beamwidth antennas, the performance of the network can be increased when using carefully designed directional antennas. Consequently, there exists an optimal operation point in terms of beamwidth to maximize the throughput of a mobile cognitive radio network with directional antennas.

II. SYSTEM MODEL

Consider a cognitive radio network of SUs, $S = \{s_1, s_2, \dots, s_n\}$. Each secondary user is equipped with a steerable directional antenna that has a beam width of σ -degrees and can be aimed with infinite granularity. Located amongst the n SUs is a set of m stationary PUs, $P = \{p_1, p_2, \dots, p_m\}$, each equipped with an omni-directional antenna, which are licensed spectrum users. We assume that the locations of the primary users are known by all secondary users. As the PUs are stationary, this information can be gathered over time as shown in [15] where multiple sensing nodes gather angle of arrival (AoA) and distance measurements over time to estimate an emitter's location. Therefore, to ensure noninterference with the PU network, we only consider the subset of point-to-point SU links to limit interference on any of the m PUs to a level below a predefined threshold, TH_{pu} .

To model the performance of a given point-to-point SU link, we must consider the expected interference level generated by other valid secondary user communication pairs. At network

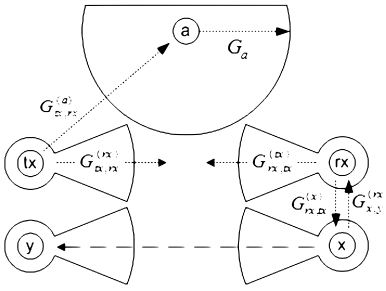


Fig. 1. Directional Antenna Gain Notation

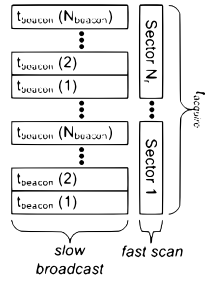


Fig. 2. Directional Neighbor Rediscovery Timing

initialization, we assume that all neighborhood information has been collected in a manner similar to [14] and that all neighbor information, including the direction of the neighbor is known.

For a given secondary user, s_{tx} , let us define the current neighbor list, N_{tx} . The neighbor list N_{tx} is a subset of the remaining $n - 1$ SUs in the network that can currently communicate with s_{tx} and, if communication is possible, this communication will not effect the performance of the local PU network. To ensure that communication between s_{tx} and one of its neighbors, s_{rx} does not interfere with the primary user network, we first estimate the expected wireless pathloss between the transmitter (s_{tx}) and a given primary receiver (p_a) using the pathloss model:

$$L_{tx,a} = \left(\frac{c}{4\pi f} \right)^2 \left(\frac{1}{d(tx, a)} \right)^l, \quad (1)$$

where $d(tx, a)$ is the distance between the users, c is the speed of light, f is the center frequency in hertz, and l is the pathloss exponent.

Based on the estimated pathloss between the users, we can estimate the interference signal strength of the transmission between s_{tx} and s_{rx} on the primary user, p_a , $a \in P$, as:

$$I_{tx,rx}^a = P_{tx} L_{tx,a} G_{tx,rx}^{(a)} G_a, \quad (2)$$

where P_{tx} is the transmission power of s_{tx} , $G_{tx,rx}^{(a)}$ is the gain of s_{tx} 's directional antenna pointed at s_{rx} in the direction of p_a , and G_a is the gain of p_a 's omnidirectional antenna. If this interference is above the pre-defined threshold TH_{pu} , then the communication between s_{tx} and s_{rx} must be disabled. To illustrate the directional antenna gains used in these equations, refer to Figure 1.

After eliminating the point-to-point SU links which could interfere with the primary user network, we must use an appropriate interference model to determine the link quality of the remaining connections. For any given SU pair, (s_{tx}, s_{rx}) , there are $(|S| - 2)$ possible interference sources that can affect signal quality. Since we are dealing with directional antennas, we must consider the transmission direction of any possible interference source with respect to the SU receiver, s_{rx} . For any pair of secondary interferers, (s_x, s_y) , we can estimate the interference on an SU communication pair, (s_{tx}, s_{rx}) as:

$$I_{tx,rx}^{(x,y)} = P_x G_{x,y}^{(rx)} G_{rx,tx}^{(x)} L_{x,rx}, \quad (3)$$

where P_x is the transmission power of the interference source s_x , $G_{x,y}^{(rx)}$ is the gain of s_x 's directional antenna facing s_y in the direction of s_{rx} , $G_{rx,tx}^{(x)}$ is the gain of s_{rx} 's directional antenna which is pointed at its neighbor s_{tx} in the direction of s_x , and $L_{x,rx}$ is the estimated wireless pathloss.

To determine the expected effect of a neighbor node s_x we must consider all of this node's neighbors as potential interference source pairs. Without loss of generality, we assume that s_x is equally likely to transmit to any of its $|N_x|$ direct neighbors. Therefore, the average interference generated by s_x transmitting to any of its neighbors on the communication pair, (s_{tx}, s_{rx}) is:

$$I_{tx,rx}^x = \frac{\sum_{i \in N_x} (I_{rx,tx}^{(x,i)})}{|N_x|} \quad (4)$$

where N_x is the neighbor list of s_x .

Here we define the activity level of a secondary user, A_x , which is the percentage of time that this user is actively transmitting to one of its neighbors. This is a tuning parameter to make the estimations of link quality in a given network scenario. Given s_x 's activity level, we can determine the expected interference of s_x on the secondary user communication pair (s_{tx}, s_{rx}) as:

$$E [I_{tx,rx}^x] = I_{tx,rx}^x A_x. \quad (5)$$

Finally, to determine the quality of a given point-to-point connection, we use the additive interference model [16] to include all potential interference sources and calculate the signal to noise and interference ratio (SINR) as:

$$\text{SINR}(tx, rx) = \frac{P_{tx} L_{tx,rx} G_{tx,rx}^{rx} G_{rx,tx}^{tx}}{N_{th} + \sum_{i \in N_{rx}} (E [I_{tx,rx}^i])}. \quad (6)$$

where N_{th} is the noise floor for the receiving SU.

Using the SINR of a given communication link, we can either determine the continuous peak sustainable data rate, or by defining a realistic set of modulation and data rate sets, we can determine, for a given network model, the expected peak data rate for any SU communication pair.

III. NEIGHBOR INFORMATION MAINTENANCE

To maintain network connectivity, the individual secondary users (SUs) must maintain a list of direct neighbors with which communication is possible and a direction for communication with each neighbor. The authors in [17] have proposed that, using a single node with multiple sector antennas, we can estimate the angle of arrival of an incoming signal within a degree of certainty defined by the Cramér-Rao bound [17]:

$$\text{CRB}(\theta) = \frac{m^{-2} \sigma_{rss}^2}{N_r \sum_{i=0}^{N_r-1} \tan^2 \left(\frac{\theta - i\Delta}{2} \right) - \left(\sum_{i=0}^{N_r-1} \tan \left(\frac{\theta - i\Delta}{2} \right) \right)^2}, \quad (7)$$

where θ is the angle of arrival estimation, N_r is the number of identical and evenly spaced antenna patterns used around a

given secondary user, m is the exponent of the *cardoid* shaped function the author's used to model a generic directional antenna pattern, and $\sigma_{r,ss}$ is the variance of the zero-mean Gaussian random noise on the communication channel.

The authors in [17] assumed that a wireless node was equipped with an switched array of sectored antennas. We can emulate this by steering our single directional antenna to a predefined set of N_r directions. It was shown in [17] that as the number of antenna elements used increases, the accuracy of the angle of arrival (AoA) estimation increases as well. Therefore, we can dynamically adjust our AoA estimation accuracy by increasing or decreasing the number of emulated sectors, N_r . By utilizing multiple, evenly spaced sectors to scan around a node, assuming an idealized model of the directional sectored antenna, a beacon transmission could be received on multiple overlapping sectors. Using more realistic models, where the antenna gain off the main lobe is non-zero, additional beacon messages could be received, increasing the accuracy of the AoA estimation.

Now that we can estimate the AoA of a direct neighbor, from a protocol standpoint, it is important to determine how we can acquire received signal strength (RSS) information for a given neighbor on each of our N_r antenna sectors. The authors in [14], [9] utilize a novel approach to discovering a network of nodes using a serialized scanning mechanism. Here, we propose utilizing a similar mechanism for neighbor rediscovery in which one of the SUs scans its N_r sectors while the other SU broadcasts a series of beaconing messages as described below.

When neighbor rediscovery begins, one of the secondary users (which can be negotiated at neighbor discovery) begins transmitting a series beaconing messages in the last known direction of the neighbor node. We refer to this as the *slow-broadcast* state. These beaconing messages contain identification information and, if successfully received by the neighbor node, will be used for RSS measurements. While the beaconing messages are being broadcasted, the neighbor SU quickly rotates its antenna in a predefined sequence of N_r directions. This is referred to as the *fast-scan* state. The rotation speed of the scanning neighbor's directional antenna should be synchronized to the beaconing broadcasts such that at most N_{beacon} messages can be received in any one direction.

After sending $N_r * N_{beacon}$ messages, the neighbor in the *slow-broadcast* state will listen for a response message from its neighbor node. If the last-known directional information was sufficiently accurate, a response control message is sent indicating that neighbor rediscovery was successful. However, if the neighbor is out of range, due to inaccurate directional information or distance, a response message will not be received, indicating that the node in the *slow-broadcast* state must expand the search for its neighbor by rotating its antenna to a different direction. How to best search for the neighbor depends on the mobility profile of the SU network. In our system, we rotate the directional antenna in an expanding search around the last known neighbor direction. For example, given an α -degree azimuth directional antenna, we first search

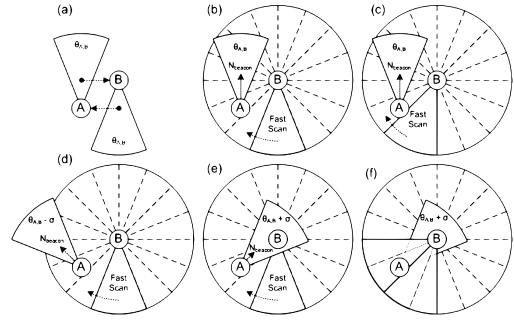


Fig. 3. Directional Neighbor Discovery

in the last known direction of the user, then on each failed rediscovery, rotate from this center α degrees at a time (i.e. $0, \alpha, -\alpha, 2\alpha$, etc.). Therefore, the time required for rediscovery is dependent on the accuracy of neighborhood information. The time required for neighbor rediscovery in a single direction is:

$$t_{acquire} = (N_{beacon} t_{beacon} N_r) + t_{respond}, \quad (8)$$

where t_{beacon} and $t_{respond}$ are the transmission times for the beaconing messages and for the neighbor's response, respectively. The timing of the neighbor rediscovery process is illustrated in Figure 2. After searching the entire azimuth around a node, if a response message is not received, it is assumed that the neighbor has moved out of communication range and the link is considered disconnected.

To initialize a neighbor rediscovery event, we define a *time-to-live* (TTL) for each neighbor table entry. This defines the amount of time we expect a given neighbor table entry will remain sufficiently accurate for communication to occur. This time is based on the expected movement profile of users in the network as well as the beamwidth of the steerable antenna. In highly mobile networks, the location information must be refreshed often to ensure that the neighbor nodes remain within range of our current direction information. Similarly, with narrow beamwidth antennas, while this would result in greater spatial diversity, the accuracy of our neighbor direction is more important as the node can more quickly move out of range.

To process of refreshing the neighbor location information is illustrated in Figure 3. Let us assume that user A and B are neighbors which have moved apart from each other and, when the TTL timer expires, they must find each other via their directional antennas. In Figure 3.a we see that the current neighbor information is inaccurate, which could result in transmission errors between users A and B. When the TTL timer expires in Figure 3.b, user A will transmit a series of ($N_{beacon} * N_r$) beaconing messages in the last known direction of user B. At the same time, user B is in *Fast-Scan* mode, rotating its directional antenna in the predefined sequence of N_r directions (Figures 3.b,3.c), attempting to acquire the AoA information for user A. Due to the inaccuracy of the directional neighbor information, the transmissions from user A are highly attenuated in the direction of user B and all beaconing messages will be lost. Therefore in Figure 3.d, user A rotates its beamwidth by σ degrees to expand the

search for user B. Finally, when user A attempts directional neighbor rediscovery in the third direction, as seen in Figure 3.e, user A’s main lobe is in the direction of user B, and a number of beaconing messages can be received and processed at user B (Figure 3.f) for AoA estimation purposes. Due to the inaccuracy of the initial directional neighbor information, in this example, three scanning sequences were required, resulting in $(3 * t_{acquire})$ seconds of search time.

IV. SIMULATION MODEL

To show the expected performance of directional antennas in mobile CRNs, we have developed a simulation suite in MATLAB. For a given simulation run, we randomly place the n SUs and m PUs in a pre-defined simulation area. Initially, we assume that all SUs have a fully populated neighbor table which includes the direction for transmission to each of its neighbors and a TTL associated with each entry in the range $(0, t_{TTL}]$.

As the simulation progresses, SUs move using a random walk profile. On each movement, the secondary user links are tested for interference with the primary user network. Those links that generate interference on any PU above the noise floor, N_{th} , are considered disconnected from the network. For each of the active point-to-point SU links, we estimate the SINR of the link based on the additive interference model described in Section II. The expected SINR is compared to a set of well known modulation schemes to determine what data rate could be sustained over the link while maintaining a bit error rate (BER) of greater than 10^{-5} . The data rates associated with the modulation schemes assume a base symbol rate of 1 mega-symbol per second [18]. The modulations used, as well as their data rate and minimum supported SINR are: {BPSK, 1Mbps, 10 dB}, {QPSK, 2 Mbps, 14 dB}, {16-QAM, 4 Mbps, 18 dB}, {64-QAM, 6 Mbps, 24 dB}.

As the simulation progresses, it is likely that some links will become disconnected either due to distance or outdated neighbor information. In either case, if, after node movement, the SINR is no longer sufficient to support communication, the link is considered disconnected until either the neighbor information can be refreshed or the nodes move back into range.

When the TTL timer expires for a given set of SUs, this link is considered disconnected for $t_{acquire}$ time as the nodes attempt to refresh their directional information. After $t_{acquire}$, if the nodes are within communication range, based on the last known directions for communication, the neighbor direction information for both SUs is updated within a degree of accuracy as defined in equation 7. If the nodes are not within communication range, the primary SU (the SU in *slow-broadcast* state), repeats the discovery process by rotating its directional antenna as described in Section II.

The state of each point-to-point link in the network is tracked in this manner for the simulation time to be post-processed for results. From this SINR and data rate information, we can determine the state of the network by finding, for any node pair, the max-min end-to-end data rate by applying

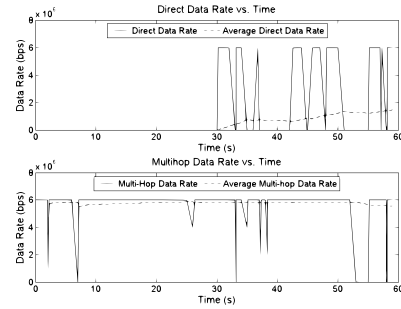


Fig. 4. Direct Link vs. Multi-hop Flow Data Rate

the Ford-Fulkerson algorithm [19]. By comparing the end-to-end paths versus direct point-to-point links we show that, though individual point-to-point links may be disconnected due to primary user locality, the network as a whole remains functional. Additionally, we can show that, due to the location of primary users in these scenarios, a secondary user network equipped with directional antennas can greatly outperform those equipped with simple omni-directional antennas.

V. RESULTS

To gather our results, we used the following parameters for all simulations, except where otherwise noted. All simulations are modeled in a 500-by-500 meter area for 60 seconds of simulated time. The 10 modeled SUs move through the simulation at a maximum speed of 20 m/s. The SU’s transmit at 0.1 watts on a 2.4GHz center frequency, 22MHz bandwidth communication channel with a pathloss exponent of 2. The SU directional antenna has a on-sector gain of 0 dBi and an off-sector gain of -60 dBi. Ten stationary PUs were modeled which utilize a 0 dBi omnidirectional antenna. For the neighbor rediscovery, we used the following values: t_{TTL} was 3 seconds, the transmission times t_{beacon} and $t_{respond}$ were 1 msec, and N_{beacon} was 5. The value of N_r is determined based on the beamwidth of the directional antenna. We ensure that the scanning sectors overlap to improve the accuracy of the AoA estimation by setting N_r to $(2 * \frac{360}{\sigma})$. To maintain non-interference with local primary users, we define the interference signal strength threshold, TH_{pu} to be the noise floor of the secondary users.

In Figure 4 we look at a single SU node pair with a antenna azimuth of 20 degrees. For the first 30 seconds of the simulation, we see that the direct data rate is zero to the presence of a primary users. However, when allowing for multi-hop communications through the SU network, we see that the data can be successfully routed to the destination node.

Figure 5 shows the relationship between beamwidth and data rate for the direct point-to-point communication link and the max-min multihop data rate through the network. When the beamwidth of the directional antenna is extremely narrow the performance of the network is degraded. Also, when neighbor rediscovery is required, the value of N_r must be high enough such that the entire azimuth about a node can be scanned. As the antenna beamwidth increases to 20 degrees, the multi-hop data rate increases due to the reduction in neighbor discovery

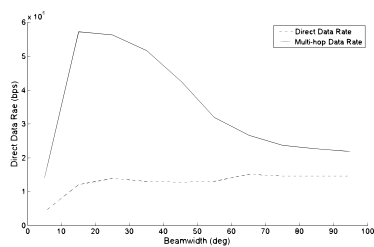


Fig. 5. Data Rate versus Antenna Beamwidth

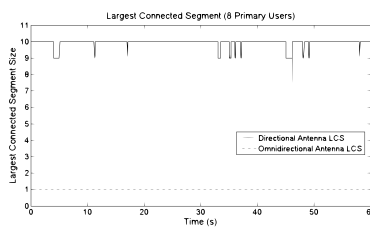


Fig. 6. Largest Connected Segment with 8 PUs

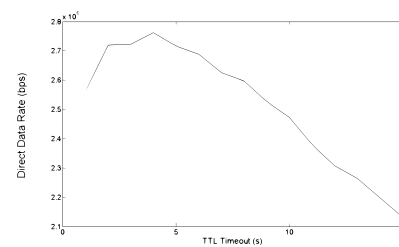


Fig. 7. Direct Data Rate vs. t_{TTL}

overhead. However, when further increasing the beamwidth, we see that, even though the overhead is further decreased, the quality of end-to-end links begins to degrade due to increased interference and links lost due to PU interference avoidance.

In Figure 6 we show the largest connected segment size of the network over time for a network consisting of eight primary users and 10 SUs with 20 degree azimuth. The largest connected segment size is the largest partition of the network in which all users can potentially communicate via direct or multi-hop transmissions. In this case, even with eight primary users in the simulation area, we see that the network is generally fully connected whereas, with omnidirectional SU antennas, we see a fully disconnected network.

In Figure 7, we show the effect that the TTL timer has on the performance of the secondary user network (with 20 degree azimuth antennas). With nodes moving at a rate of 20 meters per second, we see that a duration of between three and four seconds is a good value for t_{TTL} . With smaller values, the SUs are refreshing their neighbor information too often, leading to excessive network downtime. With larger values of t_{TTL} , point-to-point links are lost due to the mobility of the SU network. To maximize the data rate of a directional SU network, the value of t_{TTL} must be carefully chosen based on the mobility profile and directional beamwidth.

VI. CONCLUSION

In this paper, we have introduced a method for maintaining directional neighborhood information in mobile cognitive radio networks. We further highlighted the benefits of using directional antennas for CRNs even in the face of mobility. Our simulation studies confirm our expectations that directional antennas improve throughput and connectivity of CRNs in comparison with omni-directional antennas. Due to the additional overhead of maintaining direction information there exists an optimal beamwidth operation point for every mobile CRN, with given node mobility patterns, node distributions, and other parameters. Moreover, we also emphasized potential gains of using multi-hop communication in CRNs. In our future work, we will investigate analytical models to describe these trade-offs and develop protocols and algorithms that can adapt their operation to changing mobility and other system parameters.

ACKNOWLEDGMENT

This work has been supported by NSF under grant number CCF-0914912 and by Dayton Area Graduate Studies Institute (DAGSI) under contract number RY9-OSU-08-4.

REFERENCES

- [1] Federal Communications Commission, Spectrum Policy Task Force 1/8, Tech. Rep. ET Docket No. 02-155, Nov. 2002.
- [2] I. Mitola, J. and J. Maguire, G.Q., "Cognitive radio: making software radios more personal," *Personal Communications, IEEE*, vol. 6, no. 4, pp. 13–18, aug. 1999.
- [3] S. Haykin, "Cognitive radio: brain-empowered wireless communications," *Selected Areas in Communications, IEEE Journal on*, vol. 23, no. 2, pp. 201–220, feb. 2005.
- [4] I. F. Akyildiz, W.-Y. Lee, M. C. Vuran, and S. Mohanty, "Next generation/dynamic spectrum access/cognitive radio wireless networks: A survey," *Computer Networks Journal*, vol. 50, pp. 2127–2159, 2006.
- [5] A. Attar, O. Holland, M. Nakhai, and A. Aghvami, "Interference-limited resource allocation for cognitive radio in orthogonal frequency-division multiplexing networks," *Communications, IET*, vol. 2, no. 6, pp. 806–814, jul. 2008.
- [6] H. Li, D. Grace, and P. Mitchell, "Throughput analysis of non-persistent carrier sense multiple access combined with time division multiple access and its implication for cognitive radio," *Communications, IET*, vol. 4, no. 11, pp. 1356–1363, jul. 2010.
- [7] J. Nasreddine, O. Sallent, J. Perez-Romero, and R. Agusti, "Advanced spectrum management in wideband code division multiple access systems enabling cognitive radio usage," *Communications, IET*, vol. 2, no. 6, pp. 794–805, jul. 2008.
- [8] R. Murawski and E. Ekici, "Backward-compatible dynamic spectrum leasing for 802.11-based wireless networks," *GLOBECOM 2010*, Dec. 2010.
- [9] E. Felemban, S. Vural, R. Murawski, E. Ekici, K. Lee, Y. Moon, and S. Park, "Samac: A cross-layer communication protocol for sensor networks with sectored antennas," *Mobile Computing, IEEE Transactions on*, vol. 9, no. 8, pp. 1072–1088, aug. 2010.
- [10] H. Song, D. Y. Chun, and G. G. Chang, "A modified directional mac protocol for using smart antenna in wireless ad hoc and sensor networks," *WiCOM 2008*, pp. 1–3, Oct. 2008.
- [11] J. Zhang and S. C. Liew, "Capacity improvement of wireless ad hoc networks with directional antennae," *VTC 2006*, vol. 2, pp. 911–915, may. 2006.
- [12] A. Samie Ghahfarroky and F. Hendessi, "Power control and spatial reusability by using directional antenna in wireless ad hoc networks," *ICEE 2010*, pp. 220–225, may. 2010.
- [13] G. Zhao, J. Ma, G. Li, T. Wu, Y. Kwon, A. Soong, and C. Yang, "Spatial spectrum holes for cognitive radio with relay-assisted directional transmission," *Wireless Communications, IEEE Transactions on*, vol. 8, no. 10, pp. 5270–5279, oct. 2009.
- [14] E. Felemban, R. Murawski, E. Ekici, S. Park, K. Lee, J. Park, and Z. Hameed, "Sand: Sectored-antenna neighbor discovery protocol for wireless networks," in *SECON 2010*, 21–25 2010, pp. 1–9.
- [15] Z. Yang, E. Ekici, and D. Xuan, "A localization-based anti-sensor network system," *INFOCOM 2007*, pp. 2396–2400, may. 2007.
- [16] A. Iyer, C. Rosenberg, and A. Karnik, "What is the right model for wireless channel interference?" *Wireless Communications, IEEE Transactions on*, vol. 8, no. 5, pp. 2662–2671, may. 2009.
- [17] G. Giorgetti, S. Maddio, A. Cidronali, S. Gupta, and G. Manes, "Switched beam antenna design principles for angle of arrival estimation," in *EuWIT'09*, 28–29 2009, pp. 5–8.
- [18] J. C. Bicket, "Bit-rate Selection in Wireless Networks," Master's thesis, Massachusetts Institute of Technology, February 2005.
- [19] L. R. Ford and D. R. Fulkerson, "Maximal flow through a network," *Canadian Journal of Mathematics*, vol. 8, pp. 399–404, 1956.